

# We are IntechOpen, the world's leading publisher of Open Access books Built by scientists, for scientists

5,500

Open access books available

136,000

International authors and editors

170M

Downloads

Our authors are among the

154

Countries delivered to

TOP 1%

most cited scientists

12.2%

Contributors from top 500 universities



WEB OF SCIENCE™

Selection of our books indexed in the Book Citation Index  
in Web of Science™ Core Collection (BKCI)

Interested in publishing with us?  
Contact [book.department@intechopen.com](mailto:book.department@intechopen.com)

Numbers displayed above are based on latest data collected.  
For more information visit [www.intechopen.com](http://www.intechopen.com)



# Active Gaits Generation of Quadruped Robot Using Pulse-Type Hardware Neuron Models

*Yuki Takei, Katsuyuki Morishita, Riku Tazawa and Ken Saito*

## Abstract

In this chapter, the authors will propose the active gait generation of a quadruped robot. We developed the quadruped robot system using self-inhibited pulse-type hardware neuron models (P-HNMs) as a solution to elucidate the gait generation method. We feedbacked pressures at the robot system's each foot to P-HNM and varied the joints' angular velocity individually. We experimented with making the robot walk from an upright position on a flat floor. As a result of the experiment, we confirmed that the robot system spontaneously generates walk gait and trot gait according to the moving speed. Also, we clarified the process by which the robot actively generates gaits from the upright state. These results suggest that animals may generate gait using a similarly simple method because P-HNM mimics biological neurons' function. Furthermore, it shows that our robot system can generate gaits adaptively and quite easily.

**Keywords:** gait generation, interlimb coordination, pulse-type hardware neuron model (P-HNM), locomotion, quadruped robot, gait pattern

## 1. Introduction

Improvements in computer processing capability have realized advanced mobile robots [1, 2]. However, there is still no legged robot that can move flexibly enough to change our lives in a big way. One of the reasons for this is challenging to act autonomously for current control methods to instantly adapt to various events occurring in the robot's surroundings. The realization of the autonomous robot needs a higher sensory information processing system. Also, increasing the number of sensors or shorten the interval acquisition of the sensor information requires high-speed information processing. On the other hand, animals can easily act autonomously. The significant difference between robots and animals in deciding how they should act is to process all information by their brains or not. Mimicking the animal's biological system can be useful for realizing simple robot control [3, 4]. For example, the typical actions that animals unconsciously generate are respiration, chewing, and walking [5, 6]. The elucidation of generating walking action may solve the problem of current control methods for legged robots. The ordinary quadrupeds as legged animals have several locomotion patterns (gaits) [7–9]. Neurophysiology experiments have provided many insights into the characteristics

and kinematics in gait [10–18]. The finding that horses move efficiently by switching their gait to suit the situation is essential for the engineering application of their gait generation mechanisms [19]. Researchers also examined how quadrupeds generate gait [19–22]. The theory that quadruped animals unconsciously generate gaits by the interaction between the central pattern generator (CPG) and sensory inputs is widely accepted [23–26]. The variety of animals' functions makes it difficult to use their bodies to identify the essential elements required to generate gait. Although there is much discussion on the animal's gait generating mechanisms, most of it is still unclear [27, 28].

Researchers have attempted to realize CPG in engineering and use modeled CPGs to control robots [29–35]. These studies have succeeded in using the CPG models to generate locomotion, which was previously calculated by the processor [32–35]. However, how does an animal's CPGs create the gait according to the robot's surroundings is unclear. It is necessary to examine a method for generating gait employing body structure to identify the essential elements required for entities to generate gait.

Research using a biped machine with passive joints revealed that the biped machine generates a gait pattern without a control mechanism when placed on a shallow slope [36]. Another research using a quadruped machine revealed that it generates quadruped animal's gaits and switch them according to the body joints' type and the slope angle [37]. Furthermore, even if the legs' number increased to six or more, a machine generates gaits [38]. These experiments suggest that even machines without a control mechanism can generate gaits by using gravity. The finding that walking machines produce different gait depending on body structure may be related to the fact that animals have different gait for different species. Realizing a robot that can actively walk requires studying the gait generation mechanism, including the actuator's driving method.

Recently, a quadruped robot system with joints using servomotors controlled by decoupled mathematical oscillators based on the active rotator model has been proposed [39–41]. The quadruped robot's legs are controlled according to the oscillator's phase individually. Feeding back each foot's pressure to the oscillators to accelerate and decelerate the joint's angular velocity has generated the phase difference (i.e., gait). The quadruped robot could generate an animal's gait according to the pressures. Another robot controlled in the same method could switch the gaits according to its moving speed [42]. These results suggest the effectiveness of using the difference in pressure on each foot to generate gaits. Although they did not design the oscillator they used to control the joint on a biological basis, the suggestion that the reaction force the leg receives from the floor is closely related to the gait is consistent with the results of physiological experiments [16, 17].

The authors speculate that spike firing has significant roles in information processing in the nervous system. We are studying robot control using pulse-type hardware neuron models (P-HNMs) that can output the spike firing (action potential) the same as a biological neuron [43]. Our research aims to develop a simple and efficient control method for robots using the artificial motor nervous system and central nervous systems. Hardware implementation will be advantageous in a large scale network system. The authors developed a quadruped robot system that implemented an active gait generation mechanism using P-HNMs. The mechanism is similar to the peripheral nervous system in that independent P-HNMs control each limb individually [44].

This chapter describes the active gait generation method for a quadruped robot. Firstly, the authors introduce the components of our quadruped robot system. Secondly, we will discuss the gait generation method, and finally, we will show the experimental result.

## 2. Quadruped robot system

**Figure 1** shows our constructed quadruped robot system. This section describes the individual components of the quadruped robot system.

### 2.1 Mechanical and electrical components

The mechanical components of the robot system consist of the body frame and four-leg units. **Figure 2** shows the structure of the robot's body. We machined Part 1, 2, 3, and 4 from aluminum alloy sheets using the computerized numerical control (CNC) machining system and bender. Also, we formed Part A and B using a 3D printer. Part 2 and Part 3 were jointed together by Part 1 to form the body frame to connect the legs (**Figure 3**). The leg units consist of Part A, B, and two Part 4 and servomotors KRS-2552 (Kondo Kagaku co., ltd, available online at <https://kondo-robot.com/> [45]). All the leg units have the same structure. The leg length is 138 mm (from joint axis to toe), the distance between the front and rear legs is 175 mm, and the distance between the left and right legs is 101 mm. The total weight of the robot system is approximately 1.1 kg. We gave the robot system two joints for each leg, the minimum number needed to walk. This robot system has no degrees of freedom except for legs.

The robot system's electrical components consist of self-inhibited P-HNM circuit boards, pressure sensors FSR402 (Interlink Electronics, Inc., available online at <https://www.interlinkelectronics.com/> [46]), a single-board microcontroller Arduino DUE, and a peripheral circuit board. The pressure sensors have attached to the feet shown in **Figure 4**. Also, we mounted a battery and Bluetooth module to experiment without physical connections for power supply and data logging. The self-inhibited P-HNM and the peripheral circuit board are described later.

### 2.2 Self-inhibited P-HNM

The self-inhibited P-HNM consists of a cell body model and an inhibitory synaptic model. **Figure 5** shows the schematic and circuit diagram of the self-inhibited P-HNM. **Figure 5(a)** shows the connection between the cell body model and the inhibitory neuron model. A large circle represents the cell body model, and a black

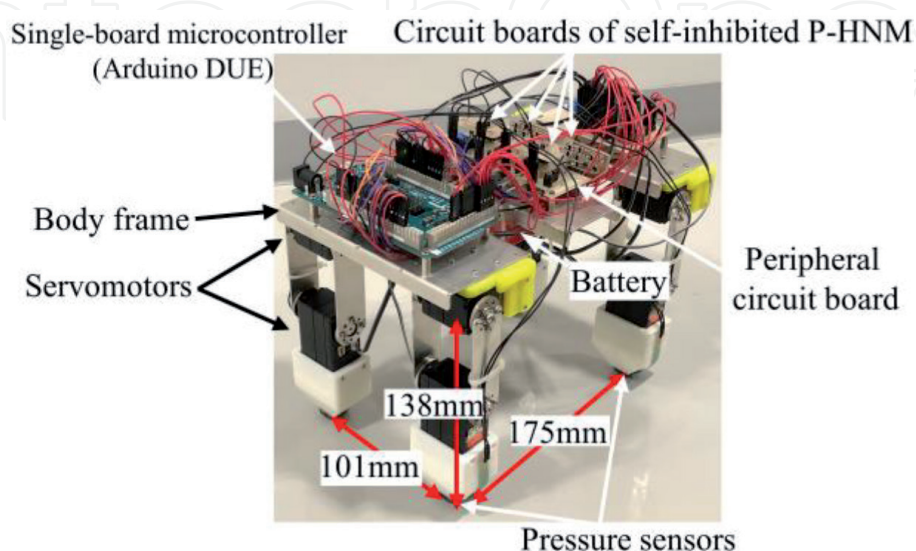


**Figure 1.**  
*Quadruped robot system.*

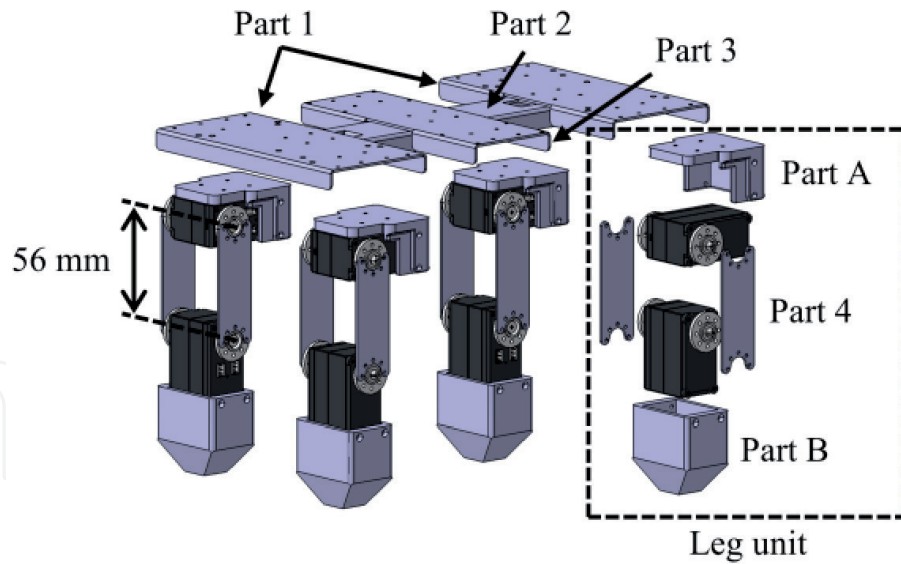


**Figure 2.** Structure of robot's body. The quadruped robot system's body consists of a body frame and four leg units.

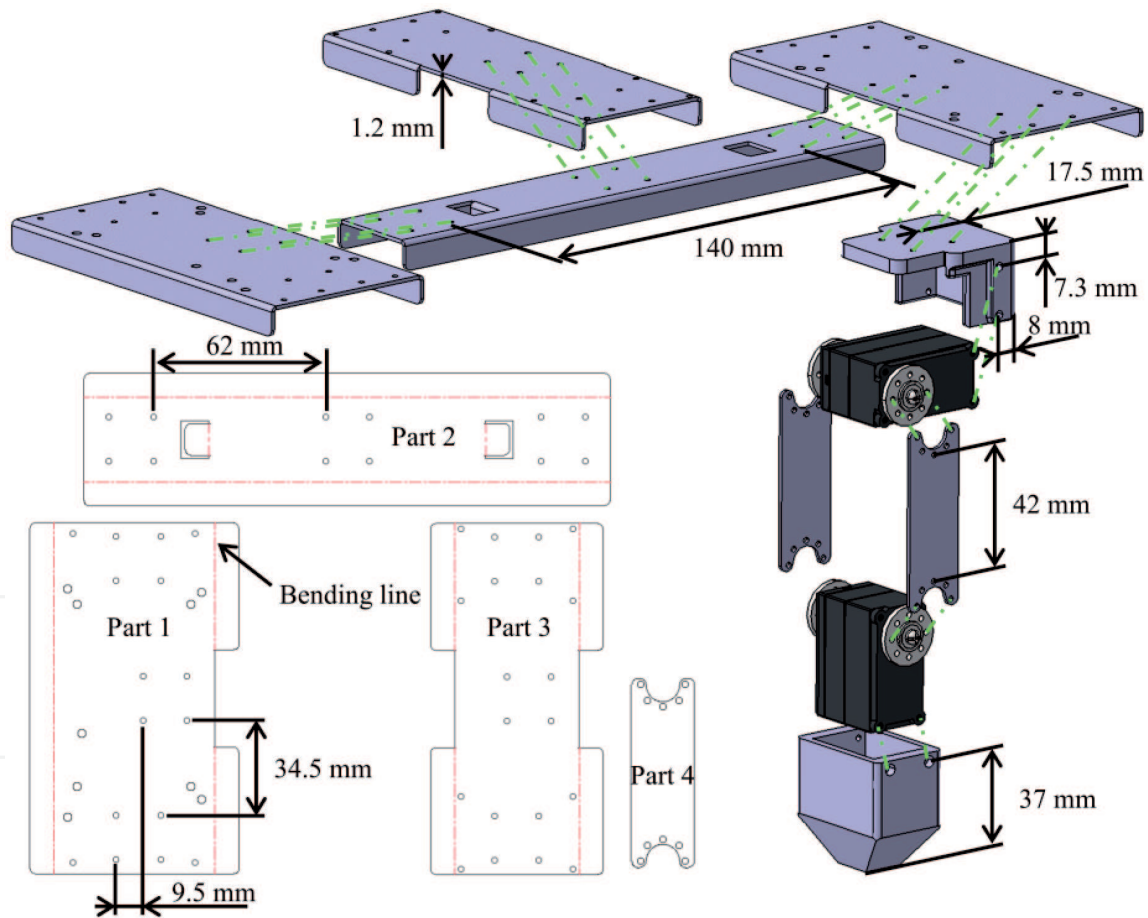


**Figure 3.** Mechanical parts of the quadruped robot system. Part 1, 2, 3, and 4 were machined using the CNC system and bender.

circle and arc representing the inhibitory neuron model. The cell body model and the inhibitory synaptic model are mimicking several functions of a biological neuron. The cell body model includes a voltage control-type negative resistance, an equivalent inductance, resistors  $R_1$  and  $R_2$ , and a membrane capacitor  $C_M$ . The voltage control-type negative resistance circuit with equivalent inductance consists of an n-channel MOSFET  $M_1$ , a p-channel MOSFET  $M_2$ , a voltage source  $V_A$ , a leak

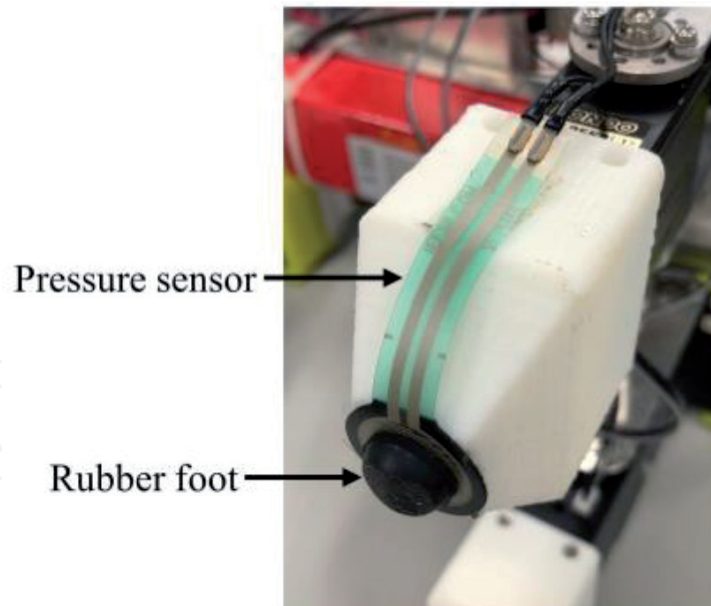


**Figure 4.**  
 Structure of each leg tip. The pressure sensor and rubber foot are attached to the end of Part B.

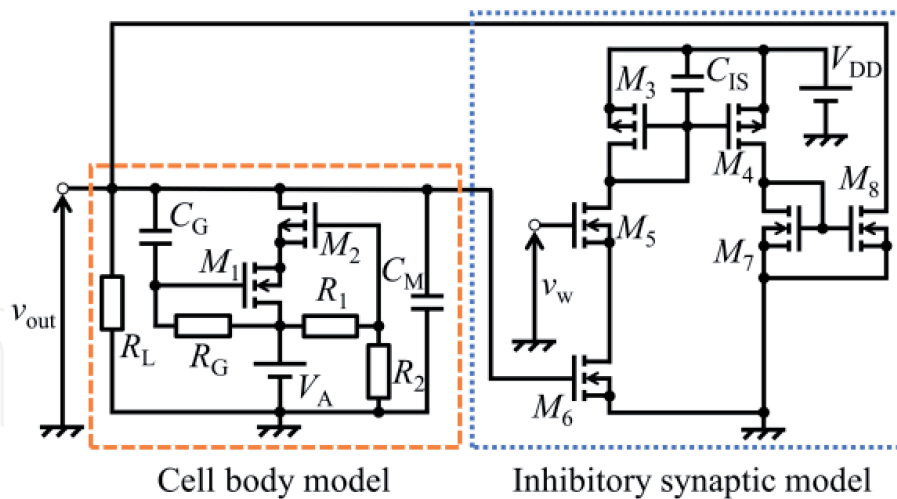
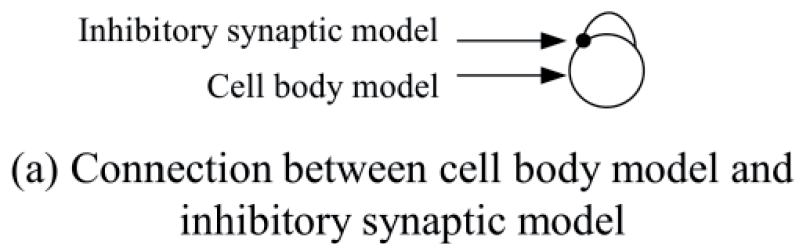


**Figure 5.**  
 Schematic diagram of self-inhibited P-HNM. According to the synaptic weight control voltage  $v_w$ , the inhibitory synaptic model inhibits the cell body model's pulse generation.

resistor  $R_L$ , another resistor  $R_G$ , and a capacitor  $C_G$ . The cell body model generates oscillating patterns of electrical activity  $v_{out}$ . More detail of the cell body model is described in [43]. The inhibitory synaptic model consists of simple current mirror circuits. The inhibitory synaptic model inhibits the cell body model's pulse generation by pulling out current from the cell body model. The strength of the inhibition can vary with synaptic weight control voltage  $v_w$ .

**Figure 6** shows the simulation result of the waveform output by self-inhibited P-HNM. We changed  $v_w$  applied to the self-inhibited P-HNM in the middle of this simulation. The circuit constants are  $C_{IS} = 3.3 \mu\text{F}$ ,  $C_G = 47 \text{ pF}$ ,  $C_M = 10 \text{ pF}$ ,  $R_1 = 15 \text{ k}\Omega$ ,  $R_2 = 20 \text{ k}\Omega$ ,  $R_G = 8.2 \text{ M}\Omega$ ,  $R_L = 10 \text{ k}\Omega$ ,  $M_{1, 5, 6, 7, 8}$ : BSS83,  $M_{2, 3, 4}$ : BSH205,  $V_{DD} = 5.0 \text{ V}$ ,  $V_A = 3.5 \text{ V}$ . **Figure 7** shows the result of the measured relation between the pulse period  $T$  and the synaptic weight control voltage  $v_w$  applied to the self-inhibited P-HNM. The curve in **Figure 8** results from approximating the plotted points with a second-order polynomial, the region we used to control the robot.

### 2.3 Leg controlling system

We connected these components to realize the quadruped robot system with an active gait generating function. **Figure 8** shows the single-leg controlling system's schematic diagram, including the peripheral circuit's circuit diagram. The outline of the peripheral circuit board and self-inhibited P-HNM circuit board is described in **Figure 9**. The peripheral circuit consists of a low-pass filter, buffer, and voltage dividing circuits. The low-pass filter consists of a resistor  $R_F$  and a capacitor  $C_F$ . The buffers consist of operational amplifier  $U_1$  and  $U_2$ . The voltage dividing circuits consist of  $R_{D1}$ ,  $R_{D2}$ , and  $R_{D3}$ . The circuit constants of peripheral circuit are  $C_F = 3.3 \mu\text{F}$ ,

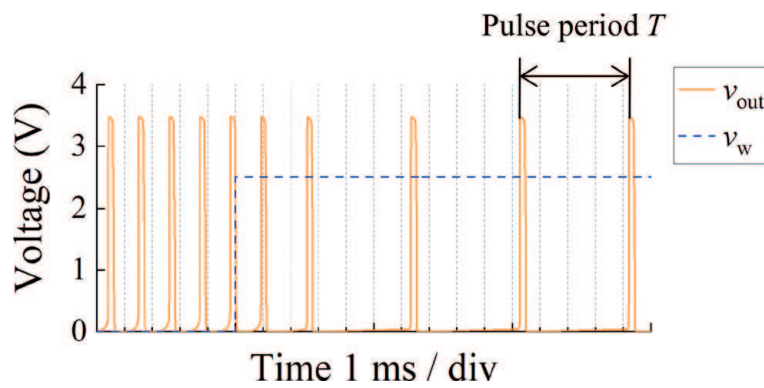


**Figure 6.** Example of self-inhibited P-HNM's output waveform (simulation result). The P-HNM outputs pulses periodically. The pulse period increases with synaptic weight control voltage  $v_w$ .

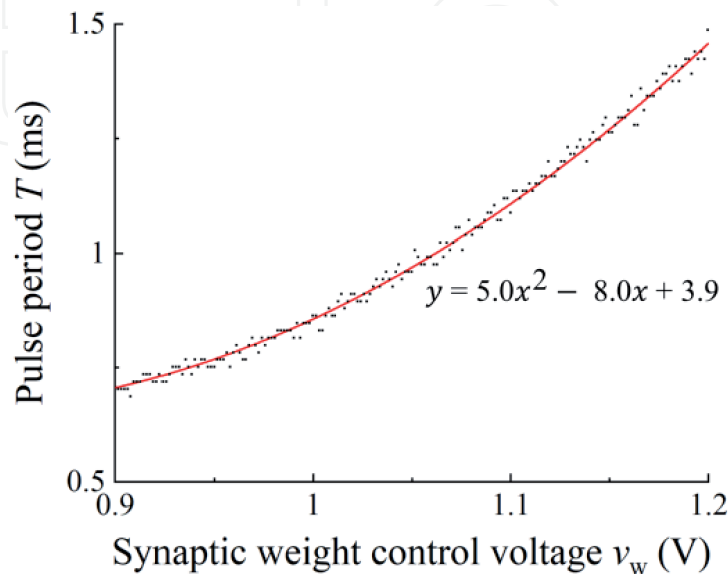


**Figure 7.** Pulse period characteristics of self-inhibited P-HNM (experimental result). The range of  $v_w$  we used to control the legs can be described in this equation.

$R_F = 11 \text{ k}\Omega$ ,  $R_{D1}, R_{D2}, R_{D3} = 11 \text{ k}\Omega$ ,  $U_{1, 2}$ : LMC6032. We input the microcontroller's PWM output to the self-inhibited P-HNM circuit boards as an analog output through the peripheral circuits' low-pass filter. We connected the self-inhibited P-HNM's output voltage to the Arduino DUE's interrupt pin through the peripheral circuit.

We set two commands in the microcontroller to move the legs individually. One is to convert the reading from the pressure sensors into the synaptic weight control voltage  $v_w$  and input it to the self-inhibited P-HNM circuit boards. The other is changing the servomotors' angle by a constant angle each time the voltage input to the interrupt pin exceeds Arduino DUE's interrupt trigger voltage (approximately 1.7 V). We defined four-foot target points to create the foot trajectory shown in **Figure 10**. The foot passes through the target points and moves along the trajectory when the robot system changes the joint's angle. We set the microcontroller to process these commands individually for four legs. The overview of these commands is shown in **Figure 11**.

Each leg moves by a constant angle each time the self-inhibited P-HNM circuit boards output a pulse and the period at which the P-HNMs output a pulse varies

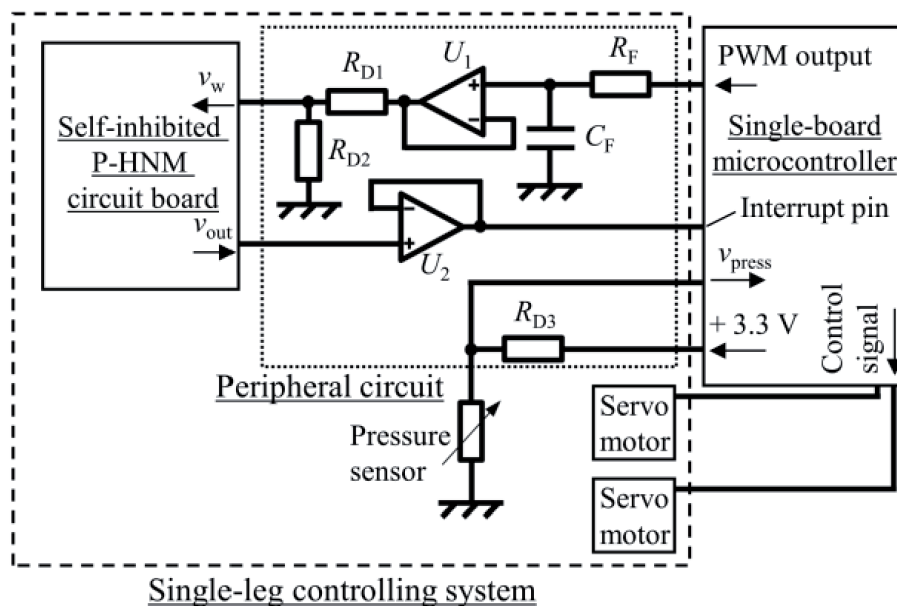


**Figure 8.** Schematic diagram of the single-leg controlling system. We implemented peripheral circuits and the self-inhibited P-HNM circuit boards to the peripheral circuit board.

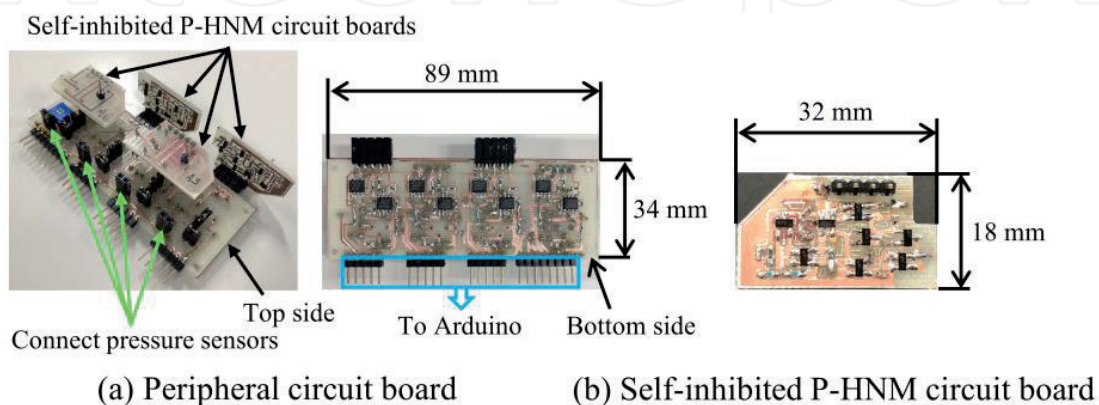


**Figure 9.** Outline of the peripheral circuit board and self-inhibited P-HNM circuit board. (a) Peripheral circuit board and (b) self-inhibited P-HNM circuit board. Four self-inhibited P-HNM circuit boards and pressure sensors are connected to the peripheral circuit board.



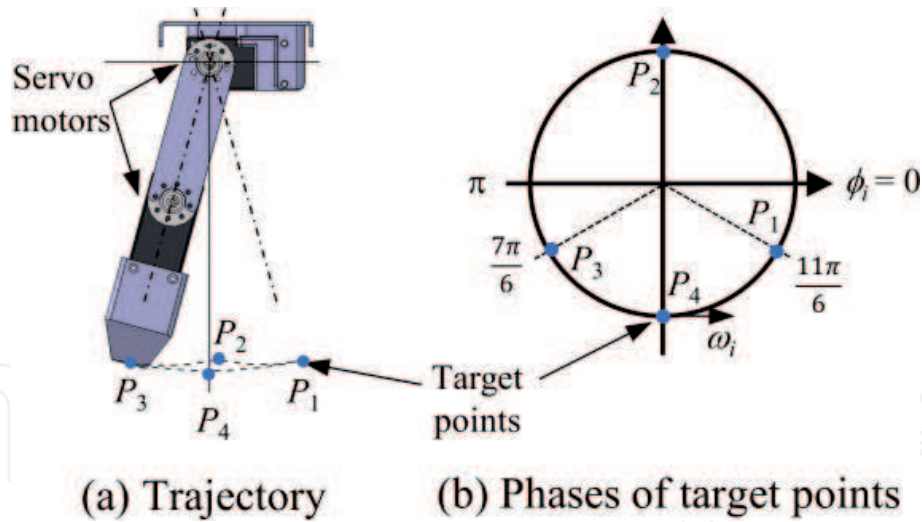


**Figure 10.** Foot trajectory. The feet draw a trajectory through target points. (a) the trajectory and (b) target point's phases.

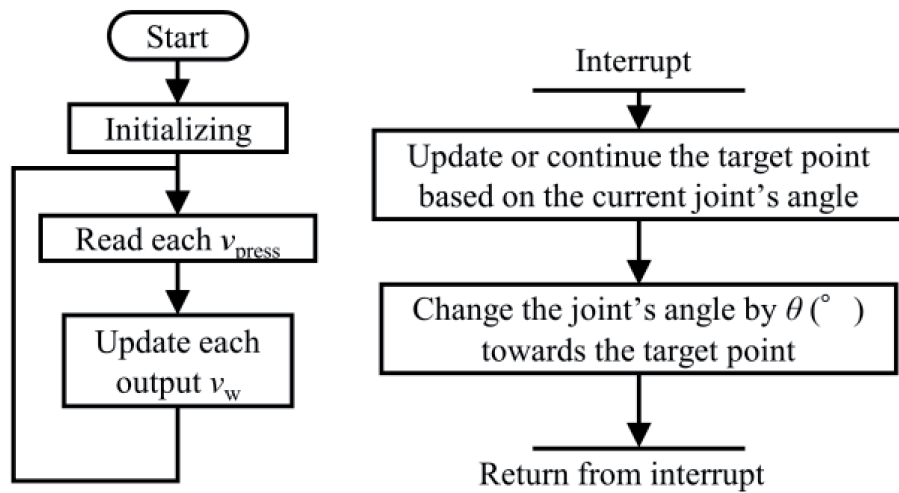


**Figure 11.** Flow chart of the set commands. Interrupt command is executed when the  $v_{out}$  output by each self-inhibited P-HNM board exceeds the interruption trigger voltage.

depending on the pressure. Therefore, the speed at which each leg of the robot moves varies depending on the pressure on the feet.

### 3. Gait generation method

The following equations express the relation between the speed of moving legs and the pressure on the feet. The microcontroller controlled the legs individually. Therefore, some parameters are different for each leg. In the following equations, the subscript “ $i$ ” means the parameter for the  $i$ th leg. The angular velocity of moving legs  $\omega_i$  can be described as the following equation:

$$\omega_i = \frac{\theta}{T_i} \quad (1)$$

where  $\theta$  is an actuation angle of servomotors each time the self-inhibited P-HNM circuit boards output a pulse. The synaptic weight control voltage  $v_w$  applied to the self-inhibited P-HNM circuit boards can be described as the following equation:

$$v_{wi} = \sigma v_{pressi} \quad (2)$$

where  $v_{pressi}$  is the applied voltage to the microcontroller depending on output by the pressure sensors.  $\sigma$  is a constant for converting  $v_{pressi}$  to  $v_{wi}$  and represents the effect of pressure. From the approximate formula in **Figure 7**, the pulse period  $T_i$  of the output voltage of self-inhibited P-HNMs  $v_{out}$  can be described as the following equation:

$$T_i = 5.0v_{wi}^2 - 8.0v_{wi} + 3.9. \quad (3)$$

From these equations,  $\omega_i$  can describe as the following equation. This equation indicates that the pressure on the foot reduces the angular velocity of moving the leg.

$$\omega_i = \frac{\theta}{5.0v_{wi}^2 - 8.0v_{wi} + 3.9}. \quad (4)$$

#### 4. Experiment result

We put the robot system on a flat floor and experimented under two conditions: the robot's walking speed is slow and fast. To change the robot's walking speed, we changed the legs' angular velocity by changing  $\theta$ . However, we did not change parameters such as  $\sigma$ . We set the initial phase of each leg to  $3\pi/2$  and let the legs to start moving at the same time.

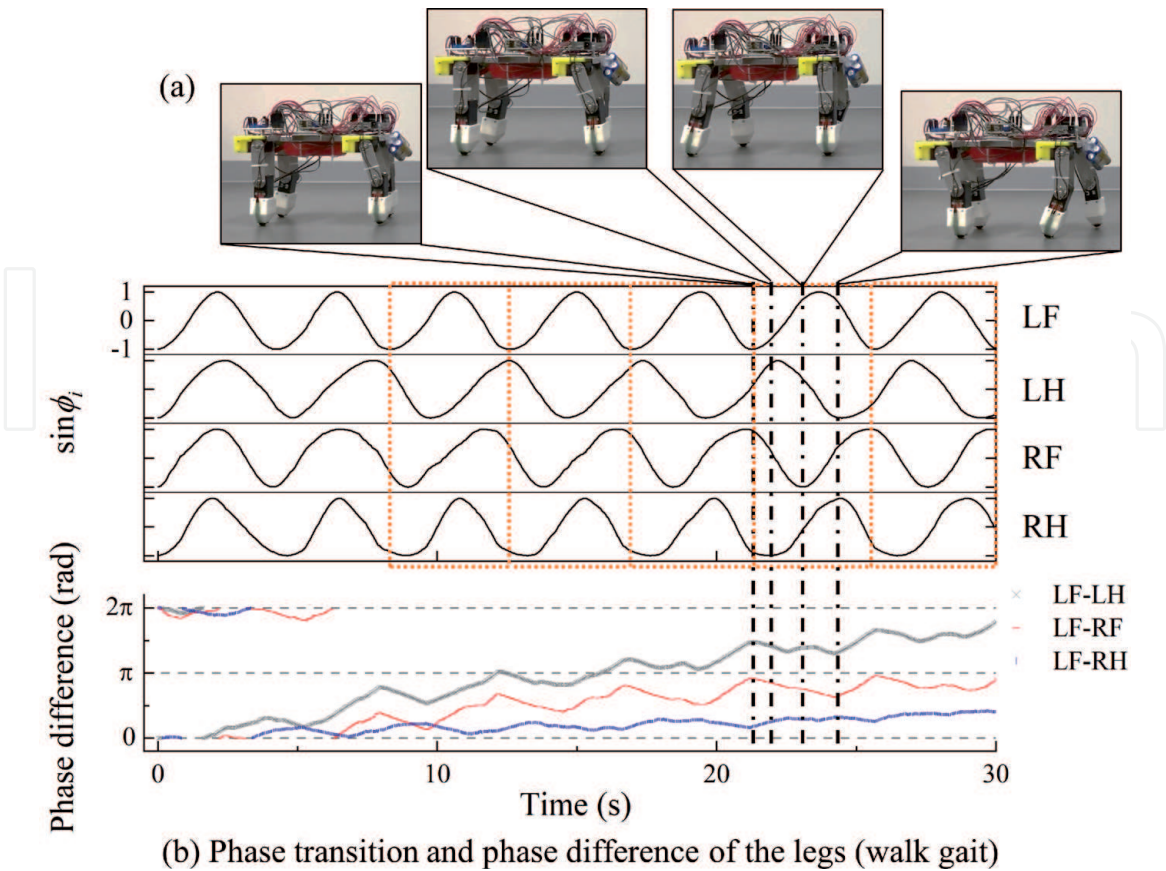


**Figure 12.** Phase transition of the legs at low speed. (a) Walking quadruped robot system and (b) each leg's phase transition and phase difference from the LF. The robot system generated the walk gait from an upright position.

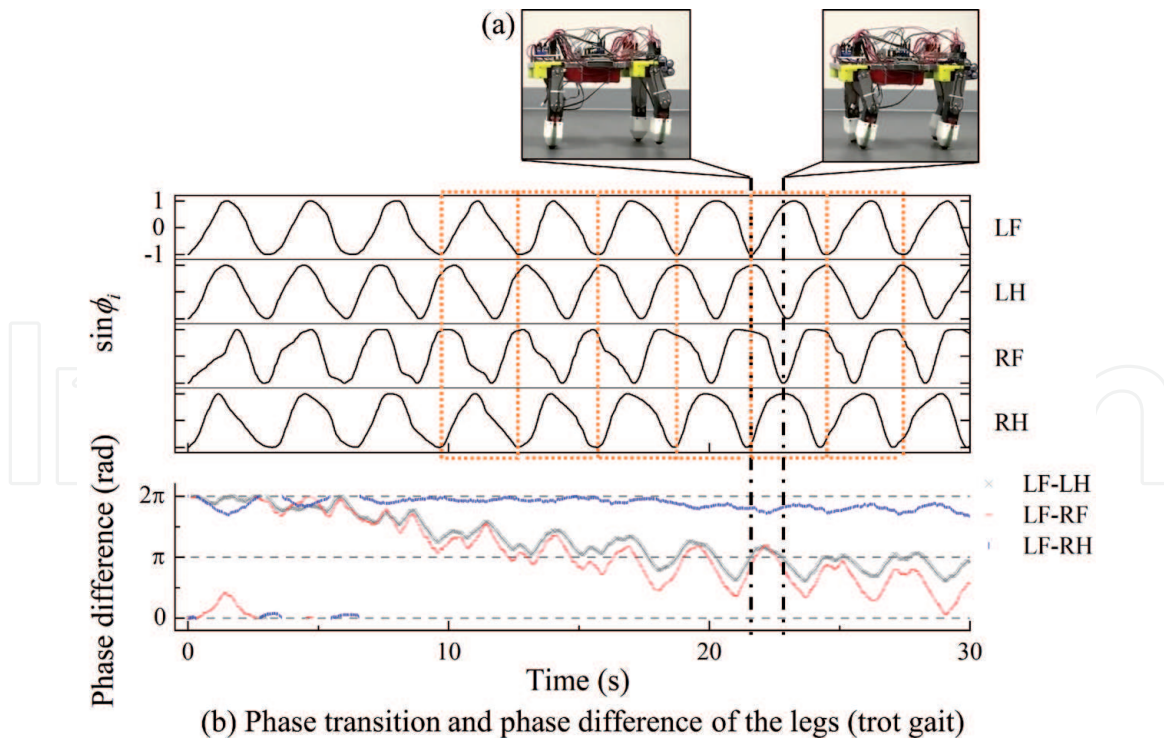


**Figure 13.** Phase transition of the legs at high speed. (a) Trotting quadruped robot system and (b) each leg's phase transition and phase difference from the LF. The robot system generated the trot gait from an upright position.

**Figure 12** shows the transition of each leg's phase  $\phi_i$ . **Figure 12** also shows the phase difference between each leg and the left foreleg at low speed. The borders in **Figure 12** mean one cycle of gait. As **Figure 12** shows from the third step after the robot system start walking, each leg's phase differences were generated around  $90^\circ$  ( $0.5\pi$  rad). Also, the order of moving the legs is left fore (LF), right hind (RH), right fore (RF), and left hind (LH), which means that this gait is the same as the horse's walk gait. In this experiment, the legs' angular velocity while the legs were not on the floor was approximately  $30^\circ/\text{s}$  ( $0.52$  rad/s). **Figure 13** shows the result at high speed. As **Figure 13** shows from the fourth step after the robot system start walking, each leg's phase difference was generated around  $180^\circ$  ( $\pi$  rad). Besides, the order of moving the legs is LF and RH, RF and LH, which means that this gait is the same as the horse's trot gait. In this experiment, the legs' angular velocity while the legs were not on the floor was approximately  $51^\circ/\text{s}$  ( $0.89$  rad/s).

These results show that the quadruped robot system can generate gaits by reducing the legs' angular velocity depending on the pressure on the feet. Also, the robot system can generate different gaits depending on moving speed. Furthermore, the characteristics of the generated gaits are similar to the horse's gaits. In our control method, we confined the change factor in each leg's speed to feedback using weight-bearing balance. Therefore, we assume that the trigger for the break in the initial phase symmetry was slightly different in the robot's weight that the limbs were supporting. We have experimentally determined the parameters such as  $\theta$  and  $\sigma$  that can stably produce these gestures. We expect that the dynamics simulator is necessary to determine these parameters quantitatively. In the future, we will use it to analyze in detail how the parameters affect the gaits.

## 5. Conclusions

In this chapter, the authors constructed a quadruped robot controlled by the active gait generating method individually for four legs. The method is simply

reducing the robot's legs' moving speed according to the pressures of feet. We implemented pulse-type hardware neuron models (P-HNMs) to the method. We conducted experiments under two conditions: when the robot's walking speed is slow and fast. As a result, the robot system actively generated phase differences of each leg. By analyzing the experimental results, we clarified the process of gait generation. Also, we confirmed that the generated phase differences were similar to the horse's gaits of walk and trot. These results suggest that quadruped robots can spontaneously generate gaits according to the environment by our proposed mechanism. Furthermore, it shows that animals may generate gait using a similarly simple method because P-HNM mimics biological neurons' function. In the future, we intend to use a kinetic simulator to determine the basis of how the robotic system generates gait.

## Video materials

Additional video materials available at: <https://bit.ly/3i91LbI>

## Acknowledgements


This work was supported by Nihon University Multidisciplinary Research Grant for (2020) and supported by Research Institute of Science and Technology Nihon University College of Science and Technology Leading Research Promotion Grant. Also, the part of the work was supported by JSPS KAKENHI Grant Number JP18K04060. The authors appreciated the Nihon University Robotics Society (NUROS).

## Author details

Yuki Takei, Katsuyuki Morishita, Riku Tazawa and Ken Saito\*  
Nihon University, Chiba, Japan

\*Address all correspondence to: [kensaito@eme.cst.nihon-u.ac.jp](mailto:kensaito@eme.cst.nihon-u.ac.jp)

## IntechOpen

© 2021 The Author(s). Licensee IntechOpen. This chapter is distributed under the terms of the Creative Commons Attribution License (<http://creativecommons.org/licenses/by/3.0>), which permits unrestricted use, distribution, and reproduction in any medium, provided the original work is properly cited. 

## References

- [1] Raibert M, Blankespoor K, Nelson G, Playter R. BigDog, the Rough-Terrain Quadruped Robot. In IFAC Proceedings; 2008. p. 10822-10825
- [2] Ruina D, Chenxing J, Ning L, Zhenjie L, Honglei Z, Bo S. The analysis of key technologies for advanced intelligent quadruped robots. In International Conference on Control and Cybernetics; 2019; Tokyo. Japan; 2019. p. 70-74
- [3] Habib MK, Watanabe K, Izumi K. Biomimetics robots from bio-inspiration to implementation. In: Proceedings of the 33rd annual conference of the IEEE Industrial Electronics Society; 5-8 November 2007; Taipei. Taiwan: IEEE; 2008. pp. 143-148
- [4] Habib MK: Biomimetics: innovations and robotics. International Journal of Mechatronics and Manufacturing Systems (IJMMS). 2011;4(2):113-134. DOI: 10.1504/IJMMS.2011.039263
- [5] Marder E, Bucher D: Central pattern generators and the control of rhythmic movements. Current Biology. 2001; 11:R986-R996. DOI: 10.1016/S0960-9822(01)00581-4
- [6] Selverston AI, Ayers J: Oscillations and oscillatory behavior in small neural circuits. Biol Cybern. 2006;95:537. DOI: 10.1007/s00422-006-0125-1
- [7] McMahon TA: The role of compliance in mammalian running gaits. J Exp Biol. 1985;115:263-282. DOI: 10.1002/jez.a.334
- [8] Yamanobe A, Hiraga A, Kubo K: Relationships between stride frequency, stride length, step length and velocity with asymmetric gaits in the thoroughbred horse. Japanese Journal of Equine Science. 1992;3:143-148. DOI: 10.1294/jes1990.3.143
- [9] Bhatti Z, Waqas A, Mahesar W, Karbasi M: Gait analysis and biomechanics of quadruped motion for procedural animation and robotic simulation. Bahria University Journal of Information & Communication Technologies. 2017;10:2.
- [10] Coulmance M, Gahéry Y, Massion J, Swett JE: The placing reaction in the standing cat: A model for the study of posture and movement. Experimental Brain Research. 1979;37:265-281. DOI: 10.1007/BF00237713
- [11] Duysens J, Pearson KG: Inhibition of flexor burst generation by loading ankle extensor muscles in walking cats. Brain Research. 1980;187(2):321-332. DOI: 10.1016/0006-8993(80)90206-1
- [12] Hoyt D, Taylor C: Gait and the energetics of locomotion in horses. Nature. 1981;292:239-240. DOI: 10.1038/292239a0
- [13] Taylor CR: Force development during sustained locomotion: a determinant of gait, speed and metabolic power. Journal of Experimental Biology. 1985;115:253-262.
- [14] Wisleder D, Zernicke RF, Smith JL: Speed-related changes in hindlimb intersegmental dynamics during the swing phase of cat locomotion. Exp Brain Res. 1990;79(3):651-660. DOI: 10.1007/BF00229333
- [15] Vilensky JA, Libii JN, Moore AM: Trot-gallop gait transitions in quadrupeds. Physiology & Behavior. 1991;50:835-842. DOI: 10.1016/0031-9384(91)90026-K
- [16] Cartmill M, Lemelin P, Schmitt D: Support polygons and symmetrical gaits in mammals. 2002;136:401-420. DOI: 10.1046/j.1096-3642.2002.00038.x

- [17] Carlo M, Biancardi, Alberto E, Minetti: Biomechanical determinants of transverse and rotary gallop in cursorial mammals. *Journal of Experimental Biology*. 2012;215:4144-4156. DOI: 10.1242/jeb.073031
- [18] Sarah J, Hilary M, Clayton M: Sagittal plane ground reaction forces, centre of pressure and centre of mass in trotting horses. *The Veterinary Journal*. 2013;e14-e19. DOI: 10.1016/j.tvjl.2013.09.027
- [19] Grillner S: Locomotion in vertebrates: central mechanisms and reflex interaction. *Physiological Reviews*. 1975;55(2):247-304. DOI: 10.1152/physrev.1975.55.2.247
- [20] Orsal D, Cabelguen JM, Perret C: Interlimb coordination during fictive locomotion in the thalamic cat. *Exp Brain Res*. 1990;82:536-546. DOI: 10.1007/BF00228795
- [21] Cruse H, Warnecke H: Coordination of the legs of a slow-walking cat. *Exp Brain Res*. 1991;89:147-156. DOI: 10.1007/BF00229012
- [22] Bertram JEA: Gait as solution, but what is the problem? Exploring cost, economy and compromise in locomotion. *The Veterinary Journal*. 2013;198:e3-e8. DOI: 10.1016/j.tvjl.2013.09.025
- [23] Grillner S, Zangger: On the central generation of locomotion in the low spinal cat. *Experimental Brain Research*. 1979;34:241-261. DOI: 10.1007/BF00235671
- [24] Frigon A, Rossignol S: Experiments and models of sensorimotor interaction during locomotion. *Biological Cybernetics*. 2006;95:607-627. DOI: 10.1007/s00422-006-0129-x
- [25] Bellardita C, Kiehn O: Phenotypic characterization of speed-associated gait changes in mice reveals modular organization of locomotor networks. *Current Biology*. 2015;25(11):1426-1436. DOI: 10.1016/j.cub.2015.04.005
- [26] Ruber L, Takeoka A, Arber S: Long-distance descending spinal neurons ensure quadrupedal locomotor stability. *Neuron*. 2016;92(5):1063-1078. DOI: 10.1016/j.neuron.2016.10.032
- [27] Delcomyn F: Neural basis of rhythmic behavior in animals. *Science*. 1980;210:492-498. DOI: 10.1126/science.7423199
- [28] Arshavdky YI, Deliagina TG, Orlovsky GN: Central pattern generators: mechanisms of operation and their role in controlling automatic movements. *Neuroscience and Behavioral Physiology*. 2016;46(6):696-718. DOI: 10.1007/s11055-016-0299-5
- [29] Yuasa H, Ito M: Coordination of many oscillators and generation of locomotory patterns. *Biological Cybernetics*. 1990;63:177-184. DOI: 10.1007/BF00195856
- [30] Ito S, Yuasa H, Luo ZW, Ito M, Yanagihara D: A mathematical model of adaptive behavior in quadruped locomotion. *Biological Cybernetics*. 1998;78:337-347. DOI: 10.1007/s004220050438
- [31] Kukikkaya R, Proctor J, Holmes P: Neuromechanical models for insect locomotion: Stability, maneuverability, and proprioceptive feedback. *Chaos: An Interdisciplinary Journal of Nonlinear Science*. 2009;19. DOI: 10.1063/1.3141306
- [32] Ishii T, Masakado S, Ishii K. Locomotion of a quadruped robot using CPG. In *IEEE International Joint Conference on Neural Networks*; 25-29 July 2004; Budapest. Hungary: IEEE; 2005. p. 3179-3184
- [33] Li X, Wang W, Yi J. Foot contact force of walk gait for a quadruped robot.

In IEEE International Conference on Mechatronics and Automation; 7-10 August 2016; Harbin. China: IEEE; 2016. p. 659-664

[34] Liu H, Jia W, Bi L. Hopf oscillator based adaptive locomotion control for a bionic quadruped robot.

In International Conference on Mechatronics and Automation; 6-9 August 2017; Takamatsu. Japan: IEEE; 2017. p. 949-954

[35] Habu Y, Yamada Y, Fukui S, Fukuoka Y. A simple rule for quadrupedal gait transition proposed by a simulated muscle-driven quadruped model with two-level CPGs. In IEEE International Conference on Robotics and Biomimetics; 12-15 December 2018; Kuala Lumpur. Malaysia: IEEE; 2018. p. 2075-2081

[36] McGeer T: Passive Dynamic Walking. *The International Journal of Robotics Research*. 1990;9(2):62-82. DOI:10.1177/027836499000900206

[37] Nakatani K, Sugimoto Y, Osuka K: Demonstration and Analysis of Quadrupedal Passive Dynamic Walking, *Advanced Robotics*. 2009;23:483-501. DOI: 10.1163/156855309X420039

[38] Sugimoto Y, Yoshioka H, Osuka K: Development of Super-multi-legged Passive Dynamic Walking robot "Jenkka-III". *SICE Annual Conference 2011; Tokyo. IEEE;2011. p.576-579*

[39] Owaki D, Kano T, Nagasawa K, Tero A, Ishiguro A: Simple robot suggests physical interlimb communication is essential for quadruped walking. *J R Soc Interface*. 2013;10(78):20120669. DOI: 10.1098/rsif.2012.0669

[40] Shinomoto S, Kuramoto Y: Phase Transitions in active rotator systems. *Progress of Theoretical Physics*. 1986;75:1105-1110. DOI: 10.1143/PTP.75.1105

[41] Shinomoto S, Kuramoto Y: Cooperative Phenomena in Two-Dimensional Active Rotator Systems. 1986;75(6):1319-1327. DOI: 10.1143/PTP.75.1319

[42] Owaki D, Ishiguro A: A quadruped robot exhibiting spontaneous gait transitions from walking to trotting to galloping. *Sci Rep* 7;2017:277 10.1038/s41598-017-00348-9

[43] Saito K, Ohara M, Abe M, Kaneko M, Uchikoba F: Gait generation of multilegged robots by using hardware artificial neural networks. *Advanced Applications for Artificial Neural Networks*. IntechOpen. 2017. DOI: 10.5772/intechopen.70693

[44] Takei Y, Morishita K, Tazawa R, Katsuya K, Saito K: Non-programmed gait generation of quadruped robot using pulse-type hardware neuron models. *Artif Life Robotics*. 2020. DOI: 10.1007/s10015-020-00637-z

[45] Kondo Kagaku co., ltd. [Internet]. Available from: <https://kondo-robot.com/> [Accessed: 2020-11-14]

[46] Interlink Electronics, Inc. [Internet]. Available from: <https://www.interlinkelectronics.com/> [Accessed: 2020-11-14]